Available online at www.sciencedirect.com

ScienceDirect

Procedia Structural Integrity 13 (2018) 1792–1797

Structural Integrity Procedia

www.elsevier.com/locate/procedia

ECF22 - Loading and Environmental effects on Structural Integrity

Stable and unstable growth of crack tip precipitates

Wureguli Reheman[a], Per Ståhle[b,*], Ram N. Singh[c], Martin Fisk[d]

[a]*Mechanical Engineering Dept., Blekinge Institute of Technology, Karlskrona, Sweden*
[b]*Solid Mechanics, LTH, Lund University, SE22100 Lund, Sweden*
[c]*Bhabha Atomic Research Centre, Mumbai-400085, Mumbai, India*
[d]*Materials science and applied mathematics, Malmö University, SE20506 Malmö, Sweden*

Abstract

A model is established that describes stress driven diffusion, resulting in formation and growth of an expanded precipitate at the tip of a crack. The new phase is transversely isotropic. A finite element method is used and the results are compared with a simplified analytical theory. A stress criterium for formation of the precipitate is derived by direct integration of the Einstein-Smoluchowski law for stress driven diffusion. Thus, the conventional critical concentration criterium for precipitate growth can be replaced with a critical hydrostatic stress. The problem has only one length scale and as a consequence the precipitate grows under self-similar conditions. The length scale is given by the stress intensity factor, the diffusion coefficient and critical stress versus remote ambient concentrations. The free parameters involved are the expansion strain, the degree of anisotropy and Poisson's ratio. Solutions are obtained for a variation of the first two. The key result is that there is a critical phase expansion strain below which the growth of the new phase is stable and controlled by the stress intensity factor. For supercritical expansion strains, the precipitate grows even without remote load. The anisotropy of the expansion strongly affects the shape of the precipitate, but does not have a large effect on the crack tip shielding.

Peer-review under responsibility of the ECF22 organizers.

Keywords: Crack tip precipitation; unstable precipitate growth; crack tip shielding; delayed hydride crack growth; stress driven diffusion.

1. Introduction

Presence of hydrogen in metals often manifests itself as loss of ductility and fracture (cf. Louthan (2008); Puls (2012)). Increased brittleness, localised plasticity, grain boundary decohesion are some examples of mechanisms that have been observed. A group of metals, e.g., zirconium, titanium, niobium, vanadium form metal hydrides, ceramics which are very brittle compared with the unaffected metal. The phenomenon causes delayed hydride cracking, DHC, observed as slow crack growth, generally accepted to be caused by hydrogen migration along the hydrostatic stress gradient and one or many hydrides growing in the crack tip vicinity. DHC is a serious problem in hydrogen based

* P. Ståhle, Tel.: +046-705539492
E-mail address: pers@solid.lth.se

2452-3216
Peer-review under responsibility of the ECF22 organizers.
10.1016/j.prostr.2018.12.359

transportation and in nuclear power plants, where zirconium is widely used for its low neutron absorption Singh et al. (2002).

The volume occupied by the metal increases with increasing concentration of hydrogen in solid solution and when a critical concentration is reached a hydride is formed accompanied by an abrupt expansion. The expansion relaxes the hydrostatic stress and releases elastic energy that drive the migration of hydrogen and the formation of hydride, cf. Turnbull (1996).

Several experimental and theoretical studies have focused on hydride formation at crack tips and its effect on strength, e.g., Bertolino et al. (2003); Cahn and Sexton (1980). Also models of crack propagation based on diffusion controlled mechanisms have been studied by Svoboda (2012); Varias and Feng (2004).

In the present work, the transport of hydrogen and the formation of expanding precipitates are modeled. The hydride growth is based on a critical hydrogen concentration. Isotropic and anisotropic expansion are compared. The hydride is assumed to be embedded in a K_I controlled stress field. The hydrogen distribution is considered to be in chemical equilibrium. The materials are assumed to have the same mechanical properties as both metal and metal hydride, with volume change as the only difference.

2. Model

First the Einstein-Smoluchowski law, Einstein (1905); Smoluchowski (1906), for stress driven diffusion is used to show that a critical hydrostatic stress is identical to a critical concentration condition for formation of hydride. After that, the hydride formation process is modelled based on a critical stress.

A large body containing a straight crack, as shown in Fig. 1, is considered. A Cartesian coordinate system x_i is attached to the crack tip. The crack occupies the region $x_1 \leq 0$ and $x_2 = 0$. Subscripts i, j, k assume values 1, 2 or 3.

The diffusive transport of hydrogen is assumed to be driven both by the negative gradient of the concentration and by the gradient of hydrostatic stress, cf. Einstein (1905); Smoluchowski (1906). The governing equation for the flux, J_i, is given as

$$J_i = -DC_{,i} + \frac{DCV}{RT}\sigma_{h,i}\,, \tag{1}$$

where D is the diffusivity constant, C is the ion/atom concentration, V is the partial molar volume, R is the universal gas constant, and T is the absolute temperature, and $\sigma_h = \sigma_{jj}/3$ is the hydrostatic stress. The writing $(\,)_{,i}$ denotes the derivative with respect to the spatial Cartesian coordinate x_i. On these Einstein's summation rule applies.

Under quasi-static conditions the flux J is negligible. Thereby, Eq. (1) is readily integrated with respect to the coordinates x_i. It is assumed that the stress in the vicinity of the crack tip is much larger than the remote stress. By putting σ_h equal to the critical stress, σ_c, one obtains the a stress equivalent to the critical concentration condition as follows,

$$\sigma_c = \frac{RT}{V}\ln\left(\frac{C_c}{C_o}\right), \tag{2}$$

where C_o is the ambient concentration at large distance away from the crack tip. A precipitate is formed or added to an already formed precipitate when the hydrostatic stress reaches the critical stress, $\sigma_h = \sigma_c$. Equivalently precipitation commence if the ambient concentration exceeds a critical value, i.e.

$$C_o = C_c \exp\left(-\frac{\sigma_h V}{RT}\right). \tag{3}$$

The total strains are decomposed into an elastic part ϵ^e_{ij} and an expansion part ϵ^s_{ij}, $\epsilon_{ij} = \epsilon^e_{ij} + \epsilon^s_{ij}$. The elastic strain is defined by Hooke's law, with a modulus of elasticity, E, Poisson's ratio ν and the expansion strain is assumed to be transversely isotropic and defined as

$$\epsilon^s_{ij} = \Lambda(\delta_{i1}\delta_{j1}e_1 + \delta_{i2}\delta_{j2}e_2 + \delta_{i3}\delta_{j3}e_1), \quad \text{where } e_1 = (1-q)\epsilon_s \text{ and } e_2 = (1+2q)\epsilon_s. \tag{4}$$

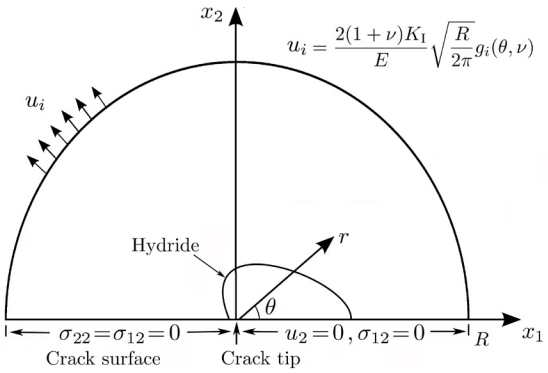

Fig. 1. Semi-infinite crack, near crack tip precipitate zone under remote mode I loading. The boundary conditions are prescribed displacements on the half circular contour, traction free crack surfaces and symmetry conditions in the crack plane ahead of the crack tip.

The e_1 and e_2 are the principal expansion strains. The largest, e_2, is assumed to be perpendicular to the crack plane $x_2 = 0$ and, hence, parallel with x_2. The parameter Λ is put to one in the precipitate and zero in the matrix material. An anisotropy parameter $0 \le q \le 1$ with $q = 0$ for isotropic materials and e.g. $q = 0.1613$ giving $e_1/e_2 = 0.634$ which is a suggested value for the ratio of the principal expansion strains of zirconium and titanium hydrides.

A hydrostatic pressure corresponding to stress free expansion, p_s, is defined as follows,

$$p_s = \frac{E}{1-2\nu}\epsilon_s\,. \tag{5}$$

Under these premisses the stress and strain distributions are obtained using an FEM. Initially the body is stress free and free from precipitates. The crack surface is traction free and the remaining remote boundary is given as a boundary layer of given displacements between the near tip region and remote constraints. The displacements are imposed at the distance R from the crack tip, see Fig. 1. Polar coordinates $r = \sqrt{x_1^2 + x_2^2}$ and $\theta = \arctan(x_2/x_1)$ are attached to the crack tip. The radius R limiting the analysed body is chosen to be around 10 times the largest extent of the precipitate, r_h. The remote constraints are applied according to mode I loading. Because of the symmetry only the upper half of the body is modelled. The imposed displacements are given by

$$u_i = \frac{2(1+\nu)K_{\rm I}}{E}\sqrt{\frac{R}{2\pi}}g_i(\theta,\nu) \;\text{ for }\; 0 \le \theta \le \pi, \tag{6}$$

where $K_{\rm I}$ is the mode I stress intensity factor and g_i are the known angular functions, cf. Broberg (1999).

2.1. Governing equations on non-dimensional form

A length unit $(\sigma_c/K_{\rm I})^2$ is used for scaling lengths, $(E\sigma_c/K_{\rm I}^2)$ is used for scaling displacements and σ_c for scaling stresses and other related quantities. On non-dimensional form the constitutive Hooke-Duhamel's equation is written,

$$\hat\sigma_{ij} = \frac{1}{1+\nu}\left\{\hat\epsilon_{ij} - \hat\epsilon^s_{ij} + \delta_{ij}\frac{\nu}{1-2\nu}(\hat\epsilon_{kk} - \hat\epsilon^s_{kk})\right\},\;\; \hat\epsilon^s_{ij} = \tilde\Lambda(1-2\nu)\left\{\delta_{ij}(1-q) + 3\delta_{i1}\delta_{j1}q\right\}\hat p_s, \tag{7}$$

and

$$\hat p_s = \frac{\hat\epsilon^s_{kk}}{3(1-2\nu)},\;\; \tilde\Lambda = \begin{cases} 1 \text{ if } \tilde\sigma_h \ge 1 \\ 0 \text{ if } \tilde\sigma_h < 1 \end{cases},\; \text{and BC's}\;\; \hat u_i = (1+\nu)\sqrt{\frac{2\hat R}{\pi}}g_i(\theta,\nu)\;\text{ on }\; \hat r = \hat R, 0 \le \theta \le \pi\,. \tag{8}$$

where $\tilde\sigma_h = (\sigma_h)_{max}/\sigma_c$, in which the $(\sigma_h)_{max}$ is the largest hydrostatic stress. Strains are defined as $\hat\epsilon_{ij} = (\hat u_{i,j} + \hat u_{j,i})/2$. Applied coordinates are the non-dimensional counterparts $\hat x_i$. As is readily observed, $\hat p_s$, q and ν are the only free

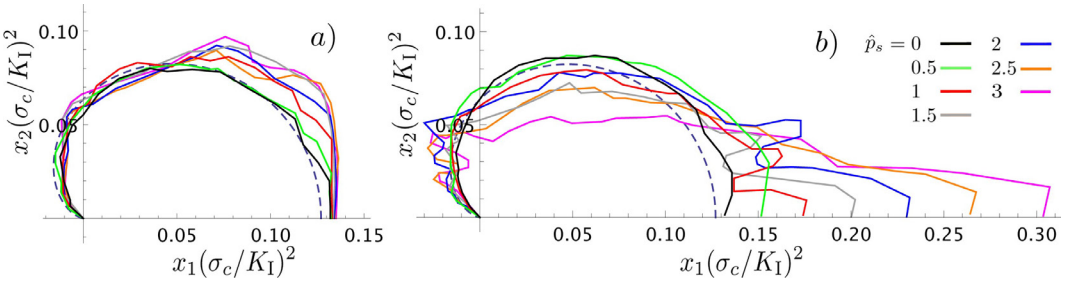

Fig. 2. The shape of precipitates for a) the isotropic ($q = 0$) and b) the anisotropic case with anisotropy factor $q = 0.16$, for different dilatation free pressure $\hat{p}_s$. The dashed curve is the exact result for $\hat{p}_s = 0$.

parameters. The equations are solved for a variation of $\hat{p}_s$ and two values of q. Poisson's ratio ν is kept the same. Apart from the expansion the mechanical properties of metal and hydride are the same.

The FE code Abaqus Hibbitt et al. (2003) is used in conjunction with a user defined subroutine that implements the mechanical behaviour of the material and keeps track of the transition from metal to hydride. The calculations are performed for variations of swelling $\hat{p}_s$. The anisotropy factor is set to $q = 0$ and $q = 0.1613$ which gives an isotropic precipitate and an anisotropic precipitate corresponding zirconium and titanium hydrides. The latter choice gives a relationship between the pricipal expansion strains of $e_1/e_2 = 0.634$, cf. Singh et al. (2007); Tal-Gutelmacher and Eliezer (2004). Poisson's ratio is set to $\nu = 0.34$, which is a suitable choice for zirconium and titanium Francois et al. (2012). The selected Poisson's ratio is also acceptable for many metals such as steel, copper, aand aluminum.

The upper half of the body, is covered by an irregular mesh consisting of 2175 four-node isoparametric plane strain elements. The linear extent of the elements near the crack tip is around $0.001\hat{R}$.

3. Results and discussion

The single physical length scale imply self-similar solutions. To confirm that the element size is sufficiently small and that the mesh is sufficiently large a range of hydride to mesh ratios is calculated. Acceptable results regarding size and shape of the hydride is found for $r_h \approx 0.1R$ for isotropic cases and $r_h \approx 0.14R$ for anisotropic cases.

The calculations are performed for five different values of $\hat{p}_s = 0$, 1, 1.5, 2, 2.5 and 3 that all a well below the critical value. The only effect induced by the precipitate on mechanical state is the material expansion. Therefore, the non-expanding case $\hat{p}_s = 0$ is identical to a case with no precipitate present.

3.1. Precipitate shapes and size

Fig. 2 shows the shape of the precipitates for isotropic a) and anisotropic b) cases for different amounts of dilatational pressure, $\hat{p}_s$. The increase of height and size should not be confused with the displacements caused by the phase transformation induced expansion strain or equivalently by the proportional dilatational pressure $\hat{p}_s$.

In the isotropic cases in Fig. 2a one observes a slight increase of hydride height in the foremost part with increasing $\hat{p}_s$. The overall influence of the expansion on the precipitate size and shape is rather small. Fig. 2b shows a with $\hat{p}_s$ increasingly wedge shaped precipitate for the anisotropic case. This is expected while a precipitate with a large expansion in the x_2 direction gives a stress concentration ahead of the precipitate and as a consequence will give a greater flux of ions/atoms to the area. The obtained shape is consistent with earlier studies, e.g., Cahn and Sexton Cahn and Sexton (1980). The obtained height to length ratio 1:16 for $\hat{p}_s = 3$ may be compared with the experimental observation by Metzger Metzger and Sauve (1996) of height to length ratios of 1:7 to 1:10. It also interesting to compare the present length of the hydride $0.31(K_I/\sigma_c)^2$ with the Dugdale Dugdale (1959) result $(\pi/8)(K_I/\sigma_c)^2 \approx 0.39(K_I/\sigma_c)^2$.

3.2. Estimate of the linear extent of the precipitate

Considering a precipitate immediately in front of a crack tip in the absence of remote load, the only relevant parameters are the dilatation free pressure p_s and the anisotropy parameter q. Let the hydrostatic stress immediately ahead of the precipitate be $\xi_o p_s$, where the positive constant ξ_o has to be dimensionless and may be a function of q and independent of p_s more than via the different precipitate shapes that are obtained for different $\hat{p}_s$. The length scale is defined by the precipitate extent, r_h, in the crack plane. Suppose now that a remote mode I load is applied. Because of the linear behaviour of the material the hydrostatic stresses of a mode I crack may be directly superimposed. In the crack plane the hydrostatic stress immediately outside the precipitate for plane strain may be written

$$\sigma_h = \xi_o p_s + \frac{2(1+\nu)}{3}\frac{K_\mathrm{I}}{\sqrt{2\pi r_h}}\,, \tag{9}$$

where the first term is the contribution from the expanding hydride and the second term is the stress caused by the crack, see e.g. Broberg (1999). To form a precipitate the hydrostatic stress must reach the critical stress, i.e. $\sigma_h = \sigma_c$. The non-dimensional form of (9) becomes,

$$1 = \xi_o \hat{p}_s + \frac{2(1+\nu)}{3}\frac{1}{\sqrt{2\pi \hat{r}_h}}\,. \tag{10}$$

where $\hat{r}_h = r_h(\sigma_c/K_\mathrm{I})^2$. Now the extent of the precipitate is obtained as,

$$\hat{r}_h = \frac{2(1+\nu)^2}{9\pi}\frac{1}{(1-\xi_o \hat{p}_s)^2}\,. \tag{11}$$

According to the result the precipitate size is uniquely determined by $\hat{p}_s$ and the constant ξ_o that is computed for vanishing remote load.

Fig. 3 shows the extent of the precipitate for different expansion stresses as the FE result and the analytical prediction. It is interesting to note that r_h is rather accurately given by Eq. (11). It is also noted the growth rate increases with increasing $\hat{p}_s$. As is readily seen in Eq. (11) the precipitate size becomes unbounded as $\hat{p}_s$ approach $1/\xi_o$ which the dilatation free pressure to around $\hat{p}_s \approx 36$ for the isotropic case and to around $\hat{p}_s \approx 6.2$ for the anisotropic case.

3.3. Crack tip Shielding

The expanded phase decreases the stresses ahead of the crack tip. The stress in the closest vicinity of the crack tip is used to compare the local crack tip stress intensity factor K_{tip} with the corresponding remote K_I for different $\hat{p}_s$. The stress intensity factor of the crack tip stress field is calculated using the relation the definition

$$K_{tip} = \lim_{x_1 \to 0} \sigma_{22}\sqrt{2\pi x_1}\,, \tag{12}$$

where the stress σ_{22} is the stress across in the crack plane inside the precipitate. Fig. 4 shows the relative stress intensity factor normalised with respect to the remote ditto versus $\hat{p}_s$. As observed the precipitate is only marginally shielding the crack tip load. For the studied case the shielding is increasing with increasing $\hat{p}_s$. It is around 10% for $\hat{p}_s = 2.5$ and obviously 0 for $\hat{p}_s = 0$. The shielding of the anisotropic material is slightly larger, which is expected since the expansion is larger in across the crack plane in this case.

4. Conclusions

The growth of an expanding precipitate at the tip of a stationary crack is studied using both analytical and numerical methods. Both phases are treated as linearly elastic with the same elastic properties. The expansion is assumed to be isotropic or anisotropic with transversely isotropic expansion. The extent of the precipitate is assumed to be small as compared with the crack length.

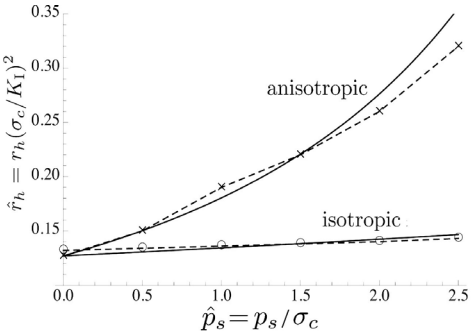

Fig. 3 Eq. (11) (dashed) compared with the FE result.,

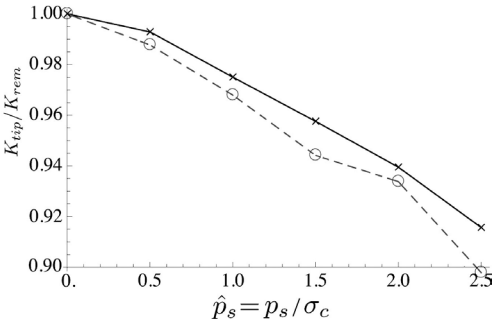

Fig. 4 The relative stress intensity factor $\hat{p}_s = p_s/\sigma_c$ for isotropic (solid) and anisotropic (dashed) materials

Direct integration of the Einstein-Smoluchowski law for stress driven diffusion shows that a critical concentration criterium for hydride growth under quasi-static conditions can be replaced with an equivalent critical hydrostatic stress, (2), or equivalently if the ambient concentration exceeds a critical value (3).

When the governingeng equations are put on non-dimensional form it is obvious that there are only three free parameters are, i.e., the expansion strain, the degree of anisotropy and Poisson's ratio, represented by $\hat{p}_s$, q and ν. The influence of Poisson's ratio is not examined.

Using that the stress immediately outside the precipitate is only mildly depending on $\hat{p}_s$, allow derivation of an analytical prediction of the precipitate size (11). The result shows that the precipitate will continue to grow even if the remote load is removed, if the dilatational free expansion $\hat{p}_s$ is sufficiently large.

Acknowledgements

Financial support from The Swedish Research Council under grant no 2011-5561 is gratefully acknowledged.

References

Louthan Jr., M.R., 2008. Hydrogen embrittlement of metals: a primer for the failure analyst. J. of Failure Analysis and Prevention, 8(3):289-307.

Puls, M.P., 2012. The effect of hydrogen and hydrides on the integrity of Zr alloy components: delayed hydride cracking, ISBN: 978-1-4471-4194-5, 452 p., Springer Science and Business Media. Berlin, Germany.

Singh, R.N., Kumar, N., Kishore, R., Roychaudhury, S., Sinha, T.K., Kashyap, B.P., 2002. Delayed hydride cracking in Zr-2.5%Nb pressure tube material. J. of Nuclear Materials, 304(2):189-203.

Bertolino, G., Meyer, G., Perez, J., 2003. Effects of hydrogen content and temperature on fracture toughness of Zircaloy-4. J. of Nuclear Materials, 320(3):272-279.

Cahn, C.D., Sexton, E.E., 1980. An electron optical study of hydride precipitation and growth at crack tips in Zr. Acta Metal., 28(9):1215-1221.

Svoboda, J., Fischer, F.D., 2012. Modelling for hydrogen diffusion in metals with traps revisited. Acta Materialia, 60(3):1211-1220.

Varias, A.G., Feng, J.L., 2004. Simulation of hydride-induced steady-state crack growth in metals-part i: growth near hydrogen chemical equilibrium. Computational Mechanics, 34(5):339-356.

Einstein, A., 1905. On the motion of small particles suspended in liquids at rest required by the molecular-kinetic theory of heat. (Über die von der molekularkin. Theorie der Wärme geforderte Bewegung von in ruhenden Flussigk. suspendierten Teilchen), Annalen der Physik, 322(8):549-60.

Smoluchowski, M., 1906. Zur kinetischen Theorie der Brownschen Molekularbewegung und der Susp., Annalen der Physik, 21(14):756-80.

Turnbull, A., Ferriss, D.H., Anzai, H., 1996. Modelling of the hydrogen distribution at a crack tip. Materials Science and Eng.: A, 206(1):1-13.

Broberg, K.B., 1999. Cracks and Fracture. ISBN:0121341305, 752 p., Academic Press, San Diego, Calif., USA.

Hibbitt, Karlsson, Sorensen, 2003. ABAQUS Theory Manual (version 6.8). Hibbitt, Karlsson and Sorenson Inc., Pawtucket, Rhode Island, USA.

Singh, R.N., Ståhle, P., Massih, A.R., Shmakov, A.A., 2007. Temperature dependence of misfit strains of δ-hydrides of zirconium. J. of Alloys and Compounds, 436(1):150-154.

Tal-Gutelmacher, E., Eliezer, D., 2004. Hydrogen-assisted degradation of titanium based alloys. Materials transactions, 45(5):1594-1600.

Francois, D., Pineau, A., Zaoui, A., 2012. Mechanical Behaviour of Materials. ISBN 978-94-007-2545-4, 646 p., DOI 10.1007/978-94-007-2545-1, Springer Science and Business Media, Dordrecht, Netherlands.

Metzger, D.R., Sauve, R.G. A self-induced stress model for simulating hydride formation at flaws. Computer technology-1996. Applications and methodology, PVP-Volume 326, Ontario Hydro Technologies, Toronto, Ontario, Canada.

Dugdale, D.S., 1959. Yielding of steel sheets containing slits. J. Mech. Physics of Solids 8:100-104.